


# DIACHRONIC ANALYSIS OF VEGETATION COVER AND SOIL DEGRADATION IN THE CENTRAL AURÈS (ALGERIA) USING MULTI-SPECTRAL REMOTE SENSING INDICES

IMANE BENBIA <sup>1</sup>, HASSEN BENMESSAOUD<sup>2</sup>, FAHIMA NEFFAR<sup>1</sup>

<sup>1</sup>Ecology and Environment Department, Faculty of Sciences and Life, Batna 2 University, Batna 05078, Algeria; e-mail: i.benbia@univ-batna2.dz

<sup>2</sup>Laboratory of Algerian Forests and Climate Change (LAFACC), Institute of Veterinary Sciences and Agronomic Sciences, Batna 1 University, Algeria

 Corresponding author

**Received:** 5 November 2025 / **Accepted:** 13 April 2026

## Abstract

Benbia I., Benmessaoud H., Neffar F.: Diachronic analysis of vegetation cover and soil degradation in the central Aurès (Algeria) using multi-spectral remote sensing indices. *Ekológia (Bratislava)*, Vol. 45, No. 1, p. 73–81, 2026.

This study examines the spatiotemporal monitoring of the vegetation cover and the processes related to soil degradation in the central Aurès region of Algeria over a 33-year period (1990–2023). Using remote sensing, GIS, and multiple spectral indices (NDVI, NDWI, BI, and SI), the analysis reveals distinct phases of vegetation regeneration and regression closely linked to anthropogenic pressures and climate change. A consistently strong positive correlation between NDVI and NDWI ( $R$  ranging from 0.76 to 0.88 across all years, peaking in 2013) highlights the significant role of soil moisture on the state of vegetation. The marked negative correlations between NDVI–BI ( $R = -0.91$ ) and NDVI–SI ( $R = -0.82$ ) show a progressive and persistent degradation of the vegetation cover, accompanied by increasing exposure of bare soils and salinization. The shift of the BI–SI correlation from negative to positive during the study period ( $-0.32$  in 1990 to  $0.60$  in 2023) indicates an ecosystemic shift toward advanced desertification. These results advocate for the urgent adoption of integrated sustainable management strategies in the Aurès Mountains.

*Key words:* Aurès massif, Landsat time series, NDVI, bare soil index, salinity index, desertification risk.

## Introduction

The central massif of the Aurès constitutes a region of major interest in terms of Mediterranean biodiversity and ecological heritage (Quézel, Médail, 2003; Bezzih et al., 2021). However, for several decades, it has been experiencing marked environmental degradation due to the combined effects of climate aridification and increased anthropogenic pressures such as intensive overgrazing, recurrent fires, and growing urbanization (Anser, 2002; Bezzih et al., 2021). These combined factors particularly weaken the most sensitive ecosystems, such as the relict forests of *Cedrus atlantica* and the maquis dominated by *Juniperus phoenicea* (Beggi et al., 2012; Laala, Alatou, 2016).

Remote sensing, and in particular spectral indices derived from Landsat images, constitutes a preferred tool for large-scale temporal and spatial environmental monitoring (Campbell, Wynne, 2011; Gorelick et al., 2017). The normalized difference vegetation index (NDVI) provides valuable information on vegetation vigor, but it alone does not precisely characterize underlying processes such as water stress, soil exposure, or salinization (Metternicht, Zinck, 2003).

To address these issues, three complementary indices were employed: the normalized difference water index (NDWI) shows changes in the humidity of soil and vegetation (Gao,

1996), the Bare soil index (BI) measures how much soil is exposed (Rikimaru et al., 2002), and the salinity index (SI) was recently tested in semi-arid areas of Algeria (Mallem et al., 2025).

Despite the ecological importance of this region, few studies have precisely quantified the spatiotemporal evolution of vegetation over the past decades. The present research aims to fill this gap by conducting a diachronic analysis of the vegetation cover in the Aurès over 33 years (1990–2023) using Landsat series and the NDVI, NDWI, BI, and SI indices. The choice of the years 1990, 2000, 2013, and 2023 corresponds to periods characterized by contrasting climatic conditions (severe droughts, wet years), thus allowing a relevant analysis of the spatiotemporal fluctuations of vegetation cover over the long term. Our approach combines image processing, GIS analysis, field survey validation, and ecological interpretation to precisely identify the phases of degradation and regeneration of vegetation cover, determine the key factors influencing these dynamics, and propose operational solutions for sustainable management adapted to this semi-arid context.

## Material and methods

The overall workflow is summarized in Figure 1.

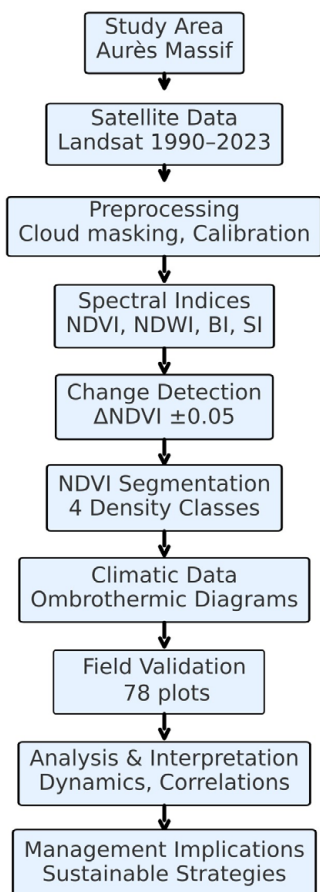


Fig. 1. Methodological workflow.

### Study area

The study area covers the mountainous core of the Aurès massif, which is situated between 35°10' and 35°30' North latitude and 5°57' and 6°39' East longitude. It encompasses the high altitudes of eight primarily mountainous communes: Théniet El Abed, Arris, Ichemoul, Foug Toub, Chir, Bouzina, Tighanimine, and Inoughissene (Fig. 2).

The calcareous-marl relief exhibits a contrasting morphology, transitioning between deeply incised valleys and tabular ridges (Benmessaoud et al., 2009). The distribution of plant ecosystems is significantly influenced by the high altitudinal variability (up to 2330 m) and the topographical heterogeneity.

The climate is semi-arid to arid, with precipitation being concentrated in the winter season and a very dry summer. This regime severely restricts the vegetative growth season and accentuates water constraints.

### Satellite data and preprocessing

This analysis utilizes four (04) series of Landsat satellite images obtained throughout the spring (from March 1 to May 31) (Table 1), a timeframe that aligns with the peak greenness phase in the study area. The selected scenes, obtained from the USGS Collection 2 – Level 2 Surface Reflectance, all exhibited cloud cover of 5% or less, thereby guaranteeing dependable interannual comparison (USGS, 2021).

Preprocessing steps included:

1. Cloud and shadow masking using the QA\_PIXEL band (bits 3 and 5).
2. Radiometric calibration by applying USGS scale factors ( $0.0000275 \times DN - 0.2$ ).
3. Spatial clipping of each image to the study boundary.

Table 1. Landsat images used in the study.

Year	Sensor	Acquisition dates	Path/Row	Spatial resolution
1990	Landsat-5 TM	Apr 15; May 29	187/034	30 m
2000	Landsat-7 ETM+	Apr 17; May 03; May 19	187/034	30 m
2013	Landsat-8 OLI	Apr 21; May 07	187/034	30 m
2023	Landsat-9 OLI-2	Apr 23	187/034	30 m

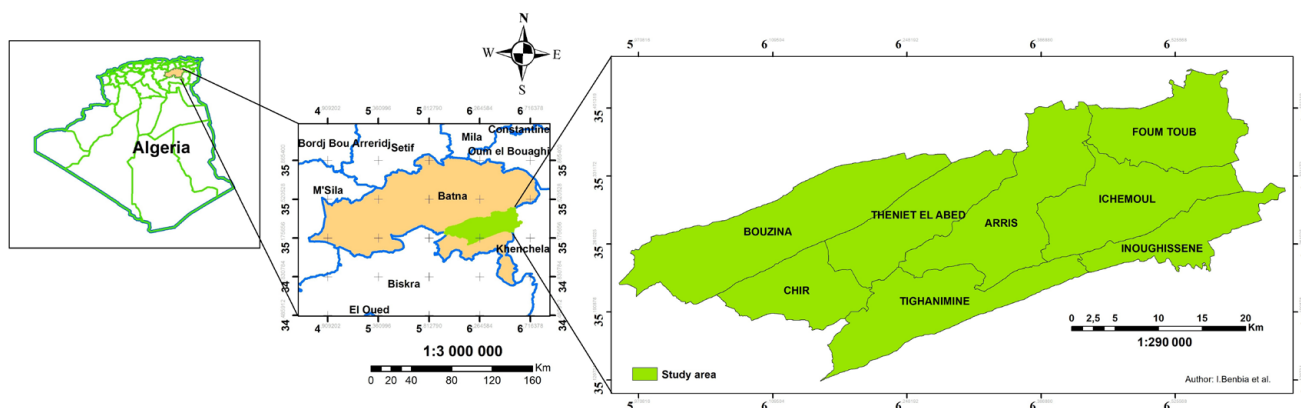


Fig. 2. Location map of the study area in the central Aurès (Algeria).

### Spectral Indices

Four spectral indices were calculated from calibrated reflectance bands:

$$1. NDVI = \frac{(NIR - RED)}{(NIR + RED)}$$

(Vigor and density of vegetation);

$$2. NDWI = \frac{(NIR - SWIR1)}{(NIR + SWIR1)}$$

(Soil and canopy moisture; Gao, 1996);

$$3. BI = \frac{(SWIR1 + RED) - (NIR + BLUE)}{(SWIR1 + RED) + (NIR + BLUE)} 100 + 100$$

(Bare soil exposure; Rikimaru et al., 2002);

$$4. SI = \sqrt{BLUE \times RED}$$

(Soil surface salinity; Mallem et al., 2025).

Each index was computed separately for TM/ETM+ (B1, B3, B4, B5) and OLI/OLI-2 (B2, B4, B5, B6) sensors (see Table 2).

### Change detection

The dynamics of vegetation cover were analyzed through diachronic comparisons of NDVI for three critical periods: 1990–2000, 2000–2013, and 2013–2023. The pairwise comparison of NDVI images over these intervals elucidates the primary patterns in vegetation dynamics and delineates regions of regression, regeneration, or ecological stability (Singh, 1989; Coppin et al., 2004). An NDVI difference map ( $\Delta NDVI$ ) was produced for each interval. A variation threshold of  $\pm 0.05$  was implemented to differentiate substantial changes from minor natural fluctuations, in accordance with the guidelines of Lunetta et al. (2006). The pixels were consequently categorized into three classes:

- **Gain:**  $NDVI > +0.05$ ;
- **Loss:**  $NDVI < -0.05$ ;
- **Stability:**  $-0.05 \leq NDVI \leq +0.05$ .

A synthesis map illustrating the changes from 1990 to 2023 has been developed to show the long-term trends in vegetation cover by consolidating all variations identified over more than three decades within the study area.

### NDVI segmentation

According to the research conducted by Khallef and Zennir (2023) on the semi-arid ecosystems of the Maghreb, NDVI values were categorized into four functional classifications representing varying degrees of vegetation cover density:

- **Dense:**  $NDVI \geq 0.50$ ;
- **Medium:**  $0.30 \leq NDVI < 0.50$ ;
- **Light:**  $0.10 \leq NDVI < 0.30$ ;
- **Bare soil:**  $NDVI < 0.10$ .

**Table 2.** Spectral bands.

Sensor	BLUE band	RED band	NIR band	SWIR 1 band
TM/ETM+	B1	B3	B4	B5
OLI/OLI2	B2	B4	B5	B6

The adoption of fixed thresholds guaranteed a rigorous temporal comparability, thereby removing biases introduced by supervised learning methods sensitive to training variations from one year to the next.

The diachronic analysis relied on quantifying the regions inhabited by each NDVI class for the reference years 1990, 2000, 2013, and 2023. The alterations between classes were subsequently assessed by cross-matrixing the categorized maps for each temporal interval (1990–2000, 2000–2013, 2013–2023) and then for the full study duration (1990–2023). This method facilitated the systematic detection of vegetative transitions, including gains (enhancements in coverage), losses (degradation), or stability. It, thus, constitutes a relevant tool for interpreting ecological evolution trajectories and diagnosing the dynamics of regeneration or regression of vegetated environments (Lu, Weng, 2007; Fichera et al., 2012).

### Climatic data

The climatic data used throughout the present study were acquired from the Batna synoptic station. The GHCN-Daily (Global Historical Climatology Network) database was used to extract daily precipitation data. These were subsequently aggregated on a monthly basis to facilitate seasonal interpretation. The seasonal dynamics were represented using ombrothermic diagrams according to the method of Bagnouls and Gaussen (1953) to characterize the interannual hydric conditions. These diagrams illustrate a relationship between the average monthly temperatures (T) (°C) and the monthly precipitation totals (P) (mm), employing the conventional scale in which 2 mm of precipitation is equivalent to 1 and the monthly precipitation totals (mm), utilizing the standard scale in which 2 mm of precipitation corresponds to 1 °C. The months meeting the criterion  $P < 2T$  are classified as dry, providing a clear visual representation of the duration and severity of the dry season for each analyzed year.

### Field validation

In order to confirm the reliability of the NDVI classification, a field validation campaign was implemented in the spring of 2023. A total of 78 floristic surveys were conducted in 200 m<sup>2</sup> sites that were distributed along an altitudinal gradient from 980 m to 2,150 m. Each point was surrounded by a 45-meter buffer zone, which corresponds to approximately 1.5 Landsat pixels, mitigated geolocation offsets and mixed-pixel effects when intersecting 30-m imagery. A stratified random sampling procedure was applied around each survey point, yielding a total of 7,020 validation pixels distributed across the four NDVI classes, following Olofsson et al. (2014). Field observations were used to support class interpretation and to validate the ecological relevance of the classification.

## Results

### Validation of the NDVI classification

The NDVI classification was assessed using 7,020 ground validation pixels. The findings demonstrate an overall accuracy of 88.2% and a Kappa coefficient ( $\kappa$ ) of 0.84. Table 3 displays the confusion matrix, which indicates the accuracy rate for each NDVI class.

### Diachronic vegetation cover dynamics

Figure 3 illustrates the geographic distribution of the four vegetation density classifications obtained from NDVI for the years 1990, 2000, 2013, and 2023. These classes relate to the following

categories: Dense, Medium, Light, and Bare soil. Table 4 provides the areas (in hectares) and the corresponding percentages for each class during these four years.

Inter-period fluctuations (Table 5) highlight three phases:

- 1990–2000: Sharp degradation (−4,972 ha Dense, −23,683 ha Medium).
- 2000–2013: Regeneration (+10,114 ha Dense, +36,813 ha Medium).
- 2013–2023: Renewed regression (−9,790 ha Dense, −32,031 ha Medium).

### Vegetation Change Dynamics ( $\Delta$ NDVI)

The spatiotemporal dynamics of vegetation cover from 1990 to 2023 were examined by a pixel-by-pixel comparison of NDVI

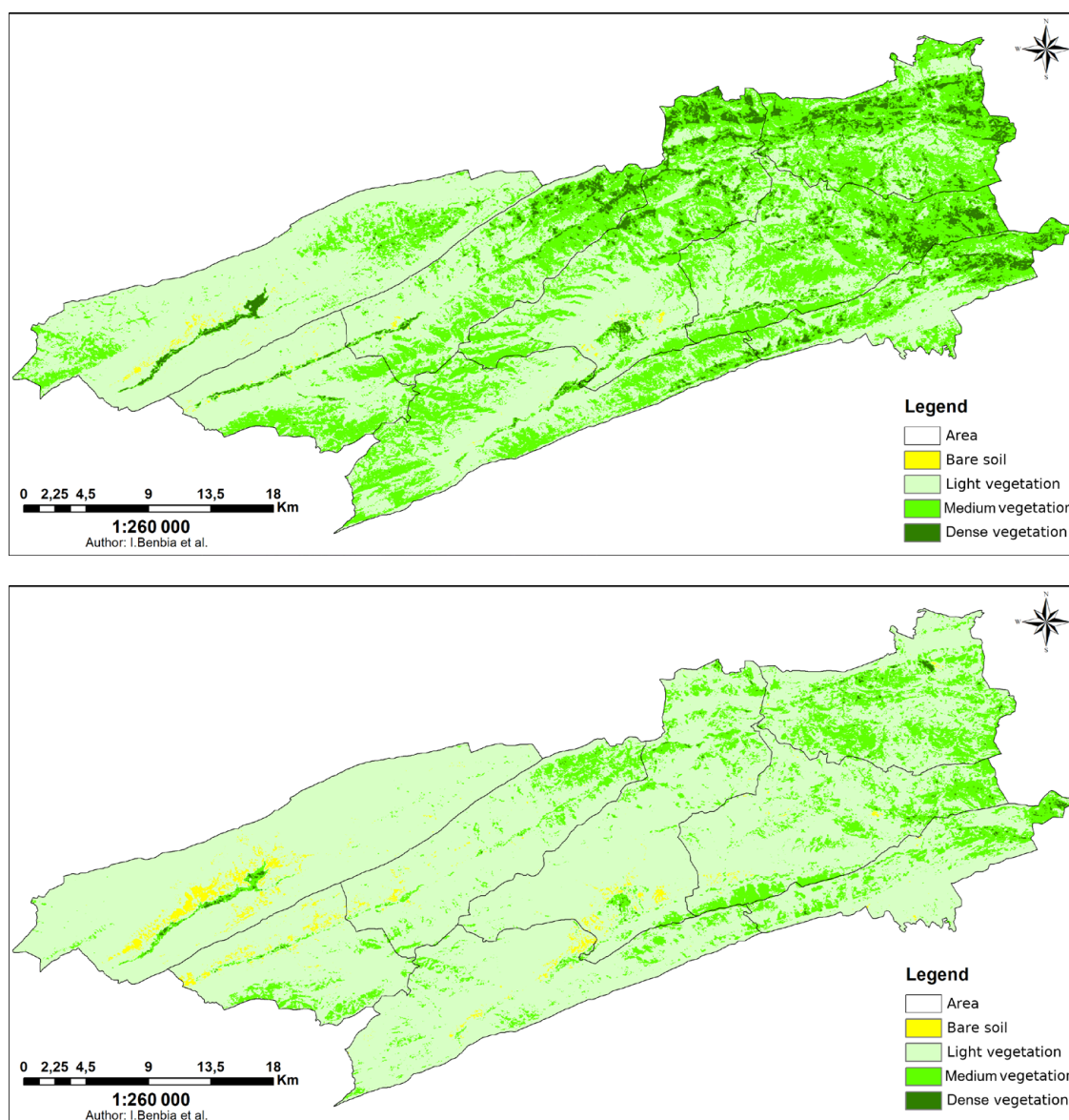


Fig. 3. NDVI maps for (up)1990 and (bellow)2000 showing four vegetation density classes (Dense, Medium, Light, Bare soil).

values. Figure 4 depicts the spatial distribution of changes throughout the study area, categorized into three classifications: Gain (in green) representing a substantial rise in NDVI; Loss (in red) denoting a reduction; and Stability (in yellow) indicating

the lack of significant change. Table 6 presents the absolute areas (in hectares) and relative areas (in percentage) corresponding to each category for the time intervals 1990–2000, 2000–2013, and 2013–2023 and for the overall global period 1990–2023.

**Table 3.** Confusion matrix and precision metrics for classification.

Reference vs prediction	Dense	Medium	Light	Bare soil	Total	Producer precision
Dense ( $\geq 0.50$ )	1,700	80	15	5	1,800	94.4
Medium (0.30–0.50)	120	1,800	150	30	2,100	85.7
Light (0.10–0.30)	20	220	1,600	60	1,900	84.2
Bare soil ( $< 0.10$ )	20	50	60	1,090	1,220	89.3
Total prediction	1,860	2,150	1,825	1,185	7,020	
User precision	91.4	83.7	87.7	92.0		

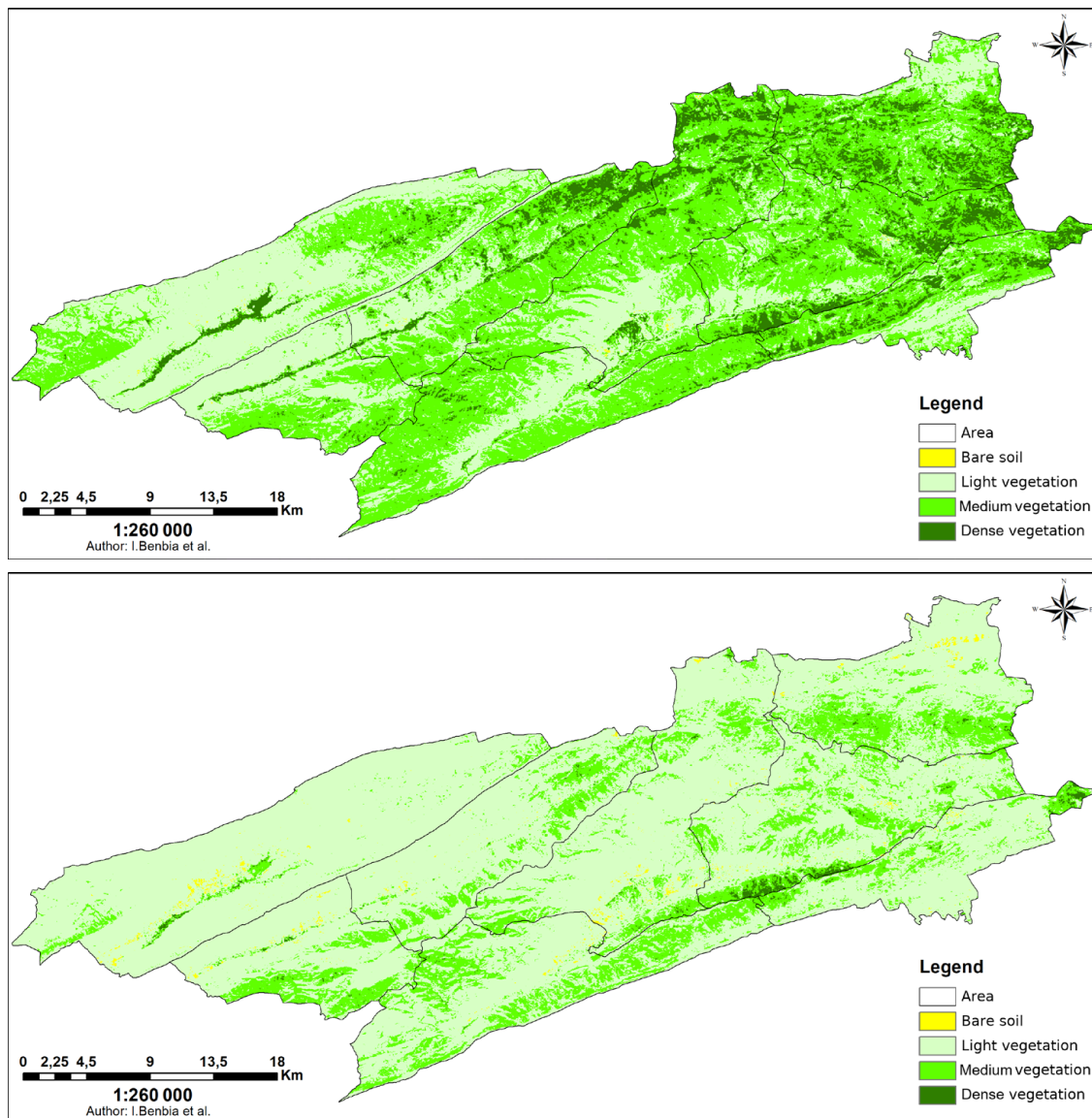


**Fig. 3.** NDVI maps for (up)2013, and (bellow)2023 showing four vegetation density classes (Dense, Medium, Light, Bare soil).

**Table 4.** Areas and percentages by NDVI class for the four years.

Year	Dense (ha/%)	Medium (ha/%)	Light (ha/%)	Bare soil (ha/ %)
1990	5,284/5.44	37,402/38.50	54,122/55.72	330/0.34
2000	312/0.32	13,719/14.12	81,545/83.95	1,562/1.61
2013	10,426/10.73	50,532/52.02	36,035/37.10	146/0.15
2023	636/0.65	18,501/19.05	77,258/79.53	744/0.77

**Table 5.** Inter-period fluctuations of the four NDVI classes.

Intervals	Δ Dense (ha)	Δ Medium (ha)	Δ Light (ha)	Δ Bare soil (ha)
1990–2000	–4,972	–23,683	+27,423	+1,232
2000–2013	+10,114	+36,813	–45,510	–1,416
2013–2023	–9,790	–32,031	+41,223	+598
1990–2023	–4,648	–18,901	+23,136	+414

**Table 6.** Absolute and relative surfaces of the Gain, Loss, and Stable categories for each interval.

Intervals	Gain (ha)	Gain (%)	Loss (ha)	Loss (%)	Stability (ha)	Stability (%)
1990–2000	319.5	0.33	34,095.8	35.10	62,723.1	64.57
2000–2013	56,163.8	57.93	376.2	0.39	40,460.0	41.68
2013–2023	187.0	0.19	47,150.0	48.54	49,663.0	51.27
1990–2023	27,039.8	27.88	29,134.9	29.99	40,825.3	42.13

**Table 7.** Pearson correlations among the spectral indices NDVI, NDWI, BI, and SI.

Year	NDVI–NDWI	NDVI–BI	NDVI–SI	BI–SI
1990	0.76	–0.44	–0.61	–0.32
2000	0.79	–0.89	–0.77	0.64
2013	0.88	–0.91	–0.71	0.45
2023	0.77	–0.86	–0.82	0.60

**Table 8.** Climate–vegetation interaction based on the  $P < 2T$  criterion (Bagnouls–Gausson).

Year	Arid months ( $P < 2T$ )	Climatic profile	Vegetation response ( $\Delta$ NDVI)
1990	7 (Mar–Sep)	Extended dry summer; annual rainfall $\approx$ 185 mm; July temperature $>$ 28 °C	Strong regression 1990–2000 (–35%)
2000	4 (Jun–Sep)	Winter precipitation (January $>$ 110 mm); favorable spring water recharge	Regeneration 2000–2013 (+58%)
2013	5 (Mar–Aug)	Balanced rainfall; secondary peak in September; moderate temperatures	Peak NDVI (Dense = 10.73 % of area)
2023	6 (May–Oct)	Irregular rainfall (May, November); summer heatwave ( $T >$ 30 °C)	Strong reduction 2013–2023 (–48%)

### Correlations among spectral indices

The examination of Pearson statistical correlations among the spectral indices NDVI, NDWI, BI, and SI indicates diverse ecological patterns across the years analyzed (1990, 2000, 2013, and 2023). Table 7 illustrates the correlation between NDVI and NDWI, highlighting the strong relationship between vegetative vigor and water availability. Furthermore, the correlations between NDVI and the BI and SI indices indicate the simultaneous deterioration of plant cover alongside soil exposure and salinization. A significant transformation is noted in the BI–SI relationship, shifting from a negative correlation in 1990 to a robust positive association in 2023.

Figure 5 illustrates the correlations between NDVI and other spectral indices, indicating that NDVI–NDWI represents the impact of surface moisture on vegetation, NDVI–BI emphasizes the disparity between vegetative vigor and Bare soil, and NDVI–SI demonstrates the detrimental effect of salinity on plant cover.

### Climate–Vegetation Relationships

The correlation between yearly climatic variations and vegetation cover dynamics was examined by the ombrothermic diagrams of Bagnouls and Gausson (1953) created for the years 1990, 2000, 2013, and 2023 (Fig. 6).

These maps illustrate the monthly distribution of average temperatures and precipitation. The monthly precipitation and temperatures documented at the Batna synoptic station were utilized to produce these diagrams.

Table 8 encapsulates the principal meteorological profiles recorded annually, the number of recognized arid months, and the associated vegetative response measured through NDVI across the specified periods.

### Discussion

#### Methodological Validation and Accuracy

The overall accuracy of 88.2% and the Kappa coefficient of 0.84 demonstrate the method’s robustness for NDVI classification (Landis, Koch, 1977). The results align with those documented by Khallef and Zennir (2023) in the Algerian steppes. The best performances were achieved for the extreme classes (Dense and Bare soil), owing to their unique spectral signatures. The confu-

sions observed between the Medium and Light classes illustrate the inherent continuity of the plant density gradient, rather than a deficiency in the approach. The method of classifying NDVI using fixed thresholds has mitigated biases linked to supervised learning, especially in heterogeneous environments.

**Vegetation Dynamics and Climatic Forcing**

The interannual analysis demonstrates significant spatiotemporal variability in the vegetation cover across the Aurès massif from 1990 to 2023. The significant reduction in dense vegetation from 1990 to 2000 (-4,972 ha) corresponds with a pronounced aridification period and heightened human-induced stressors (Beghami et al., 2012; Bezzih et al., 2021). In contrast, the period from 2000 to 2013 exhibits an important regeneration phase (+10,114 hectares of dense vegetation), likely enhanced by improved climatic circumstances, particularly increased spring water recharge (Table 8). The notable reduction in dense vegetation

from 2013 to 2023 (-9,790 ha) indicates a revival of pressures, particularly associated with increased summer aridity and human-induced disturbances.

The NDVI difference map from 1990 to 2023, along with the absolute and relative areas of the Gain, Loss, and Stable classes for each interval, reveals three significant trends: (i) substantial degradation from 1990 to 2000 (35% of the area in loss), (ii) localized regeneration from 2000 to 2013, and (iii) a new phase of rapid decline from 2013 to 2023. The increase recorded from 2000 to 2013 (about 56,164 ha) corresponds with a comparatively moist and stable interval. Nevertheless, the recent loss of 47,150 hectares may indicate a resurgence of active desertification processes. These results corroborate the research of Giorgi and Lionello (2008) about the vulnerability of Mediterranean plant cover to climate change.

The examination of ombrothermic diagrams indicates a strong association between the intensity of the dry season and the vegetation’s reaction. In 1990 and 2023, vegetation saw a

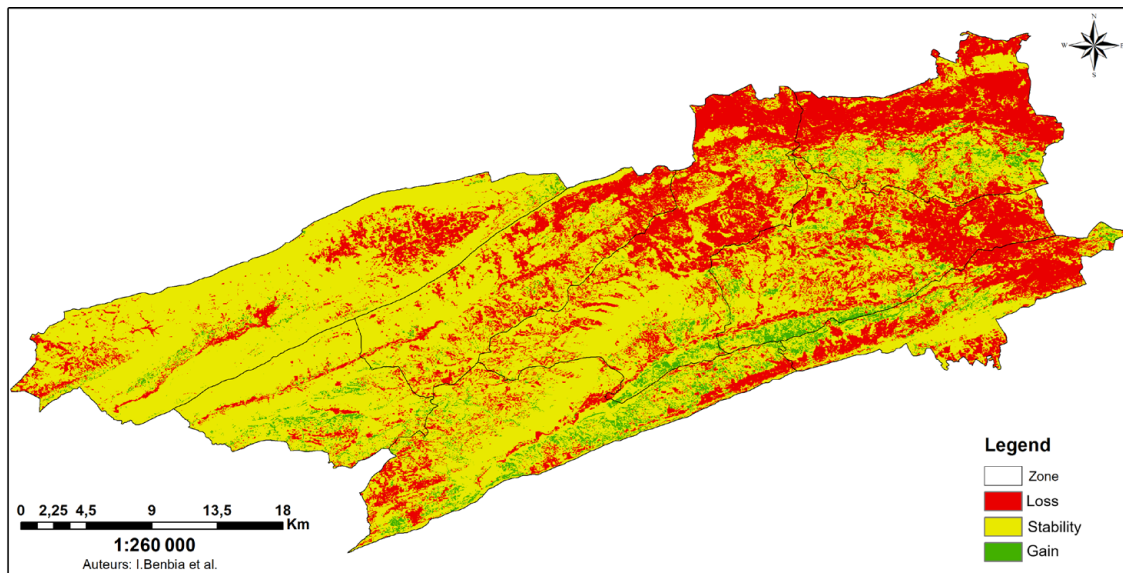


Fig. 4. NDVI change map ( $\Delta$ NDVI) between 1990 and 2023, showing Gain, Loss, and Stability classes.

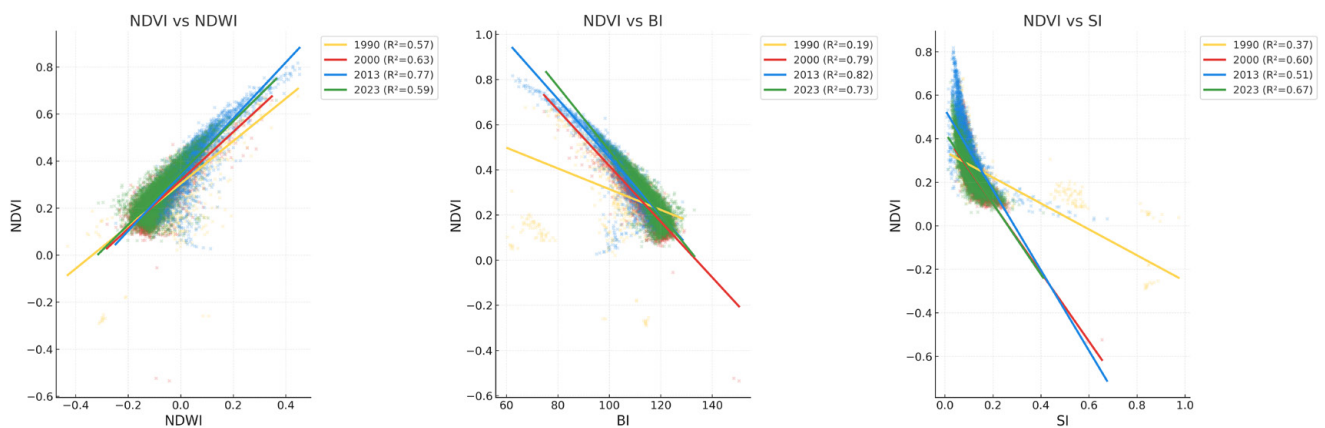
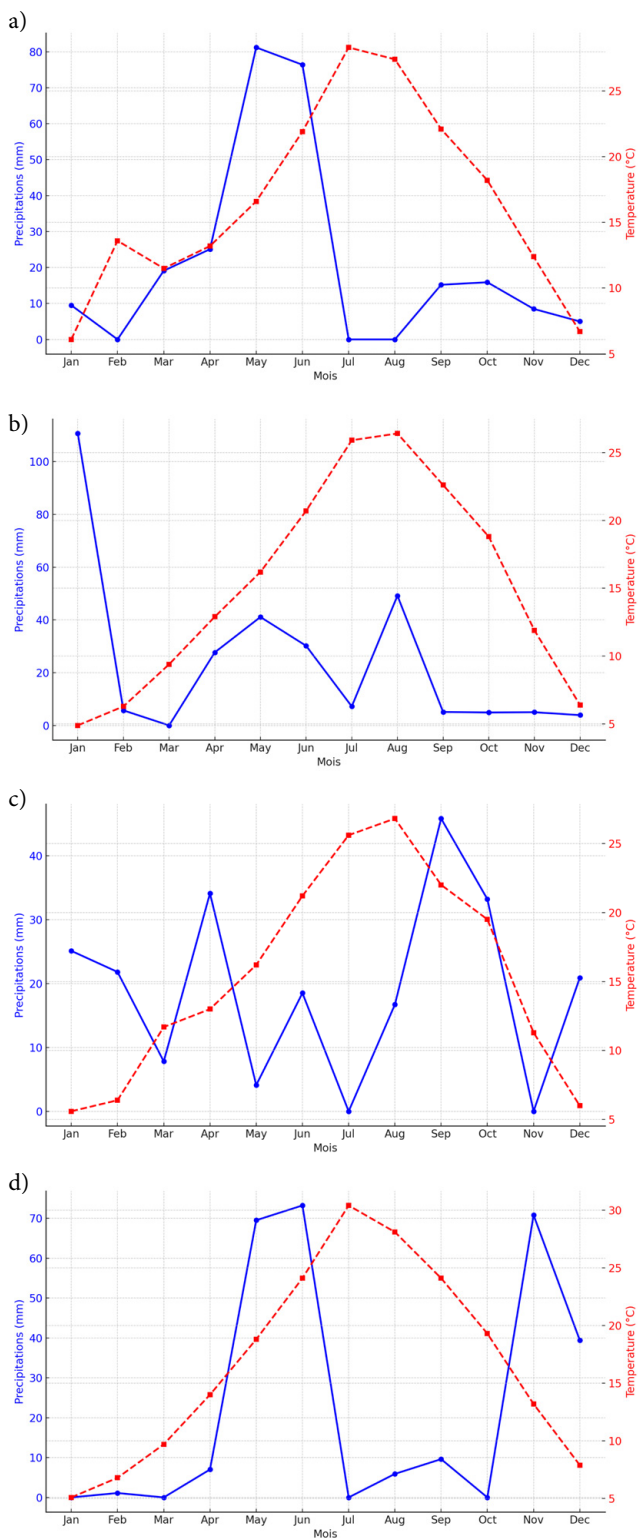


Fig. 5. Relationships between NDVI and the other spectral indices (NDWI, BI, and SI).



**Fig. 6.** Ombrothermic diagrams (Bagnouls–Gausson) for (a) 1990, (b) 2000, (c) 2013, and (d) 2023 at the Batna synoptic station.

substantial reduction due to extended water stress (7 and 6 dry months, respectively). Conversely, the years 2000 and 2013 exhibit a more evenly distributed rainfall pattern and moderate

summer temperatures, circumstances favorable for a partial restoration of vegetation cover (Quézel, Médail, 2003). These data indicate that the NDVI is a sensitive metric of seasonal water availability and the durability of extreme events.

### Ecological Insights from Spectral Indices

The analysis of correlations across spectral indices (NDVI, NDWI, BI, and SI) demonstrates strong and dynamic ecological interactions throughout the examined period. The strong positive association consistently seen between NDVI and NDWI (R reaching 0.88 in 2013) substantiates the significant impact of water availability on vegetation vitality in the central Aurès region. The results align with the research of Gao (1996) and Mallem et al. (2025), emphasizing the critical role of moisture in sustaining vegetation cover in a semi-arid Mediterranean ecosystem. When hydrological conditions enhance, a considerable rise in photosynthetic activity and plant biomass is seen, especially during the regeneration phase from 2000 to 2013.

The pronounced negative correlations observed between NDVI and BI (R as low as  $-0.91$  in 2013) and between NDVI and SI (R as low as  $-0.82$  in 2023) indicate a substantial deterioration of vegetation cover alongside a marked rise in Bare soils and salinization. These adverse correlations are indicative of advanced degradation processes, seen in other semi-arid Mediterranean habitats experiencing significant anthropogenic pressures (Laala, Alatou, 2016). Significant vegetation losses over the key decades of 1990–2000 and 2013–2023 closely coincided with bouts of extended drought.

The BI–SI correlation exhibited a significant transformation, shifting from a negative value of  $-0.32$  in 1990 to a notable positive value from 2000 onward, registering  $+0.64$  in 2000 and  $+0.60$  in 2023. This reversal indicates a significant change in ecosystem dynamics: initially, salinized regions were not inherently barren, but as degradation escalates, the processes of salinization and denudation become closely linked, demonstrating a gradual decline in the physical (texture, structure) and chemical (salt accumulation) characteristics of the soils. This ecological transition toward degradation signifies significant deterioration, with desertification processes accelerating systematically and permanently if prompt remedial actions are not implemented (Mallem et al., 2025).

### Implications for Sustainable Management

The sensitivity of NDVI to winter–spring precipitation shortfalls, previously emphasized in other semi-arid Mediterranean areas (Gouveia, Trigo, 2008; Vicente-Serrano et al., 2020), necessitates the establishment of an early warning system that combines monthly rainfall monitoring and high-resolution satellite imagery. The warning threshold can be set at a decrease in NDVI of greater than 0.05 between two decadal composites (10 days), triggering targeted field inspections (Gorelick et al., 2017).

The swift conversion of initially designated “Medium” regions to “Light” in dry years highlights the necessity to regulate the animal population on vulnerable slopes. Three-year rotational grazing and temporary closures of at least 20% of the most degraded areas are recommended in accordance with the guidelines established for semi-arid regions (Zdruli, Zucca, 2023).

The spontaneous regeneration centers identified from 2000 to 2013 suggest that assisted restoration may depend on xerotolerant species like *Pinus halepensis* and *Pistacia atlantica*, which can sustain an NDVI exceeding 0.35 in arid conditions (Bezzih et al., 2021). Selective thinning and protection from grazing facilitate the recovery of relict cedar woods (*Cedrus atlantica*).

The latest NDVI declines correspond with a rise in fire frequency (Bezzih et al., 2021). Establishing linear firebreaks, implementing brush clearing via targeted grazing, and employing thermal drones for swift fire detection are key strategies. The creation of small hill ponds and contour benches on bare hillsides enhances water retention and mitigates erosion (Lu, Weng, 2007).

These actions, in conjunction with monitoring, regulated pastoral management, focused ecological restoration, and fire and water management, establish a framework to reverse vegetation decline and enhance the resilience of the central Aurès massif against anticipated aridification.

## Conclusion

This work allows a 33-year analysis of the spatiotemporal dynamics of vegetation cover in the central Aurès region by the integration of Landsat satellite imagery, spectral indices (NDVI, NDWI, BI, and SI), climate data, and field surveys. The results indicated a succession of degradation and regeneration stages, closely associated with climate variations, particularly the length and severity of arid intervals.

The reduction in vegetation cover noted between 1990–2000 and 2013–2023 highlights the growing susceptibility of this mountainous environment to climate aridification and unregulated human activities, particularly overgrazing, fires, and urbanization. Conversely, the period from 2000 to 2013, marked by enhanced spring water recharge, demonstrates the persistence of vegetation under improved ecological conditions.

The threshold-based NDVI classification method validated through field surveys, achieved high overall accuracy, thereby enhancing the reliability of ecological interpretations.

Furthermore, the ombrothermic diagrams validated that the criterion  $P < 2T$  continues to be pertinent for associating water stress with vegetative vigor. These findings necessitate a more cohesive and flexible management approach for the Aurès domains, including measures such as reforestation, curtailing overgrazing, safeguarding relict regions, and enhancing water retention. The integration of spectral indices (NDVI, NDWI, BI, and SI) with climate analysis is validated as a crucial tool for ecological monitoring and the formulation of conservation strategies in Mediterranean mountainous regions.

## References

Anser, A. (2002). L'Aurès oriental: Un milieu en dégradation. *Journal Algérien des Régions Arides*, 1, 24–32.

Bagnouls, F. & Gaussen H. (1953). Saison sèche et indice xérothermique. *Bull. Soc. Hist. Nat. Toulouse*, 88, 193–239.

Beghami, Y., Kalla, M., Thinon, M. & Benmessaoud H. (2012). Spatiotemporal dynamics of forest and mountain formations in Aurès Area, Algeria. *Journal of Life Sciences*, 6(6), 663–669. DOI: 10.17265/1934-7391/2012.06.012.

Benmessaoud, H., Kalla, M. & Driddi H. (2009). Évolution de l'occupation des sols et désertification dans le sud des Aurès (Algérie). *M@ppemonde (En ligne)*, 94, 1–11.

Bezzih, H., Malki, H. & Aissi A. (2021). Characterising of plant cover evolution in the Aurès region (eastern Algeria): Using Landsat imagery. *Geoadria*, 26(2), 111–124. DOI: 10.15291/geoadria.3203.

Campbell, J.B. & Wynne R.H. (2011). *Introduction to remote sensing*. Guilford Press.

Coppin, P., Jonckheere, I., Nackaerts, K., Muys, B. & Lambin E. (2004). Digital change detection methods in ecosystem monitoring: A review. *Int. J. Remote Sens.*, 25(9), 1565–1596. DOI: 10.1080/0143116031000101675.

Fichera, C.R., Modica, G. & Pollino M. (2012). Land cover classification and change-detection analysis using multi-temporal remotely sensed imagery and landscape metrics. *European Journal of Remote Sensing*, 45(1), 1–18. DOI: 10.5721/EuJRS20124501.

Gao, B. (1996). NDWI—A normalized difference water index for remote sensing of vegetation liquid water from space. *Remote Sens. Environ.*, 58(3), 257–266. DOI: 10.1016/S0034-4257(96)00067-3.

Giorgi, F. & Lionello P. (2008). Climate change projections for the Mediterranean region. *Global and Planetary Change*, 63(2–3), 90–104. DOI: 10.1016/j.gloplacha.2007.09.005.

Gorelick, N., Hancher, M., Dixon, M., Ilyushchenko, S., Thau, D. & Moore R. (2017). Google Earth Engine: Planetary-scale geospatial analysis for everyone. *Remote Sens. Environ.*, 202, 18–27. DOI: 10.1016/j.rse.2017.06.031.

Gouveia, C. & Trigo R.M. (2008). Influence of climate variability on wheat production in Portugal. In A. Soares, M.J. Pereira & R. Dimitrakopoulos (Eds.), *geoENV VI – Geostatistics for Environmental Applications. Quantitative Geology and Geostatistics*, vol. 15 (pp. 335–345). Dordrecht: Springer. DOI: 10.1007/978-1-4020-6448-7\_28.

Khallef, B. & Zennir R. (2023). Forest cover change detection using Normalized Difference Vegetation Index in the Oued Bouhamdane watershed, Algeria – A case study. *J. For. Sci.*, 69(6), 254–265. DOI: 10.17221/192/2022-JFS

Laala, A. & Alatou D. (2016). Analyse de la dynamique des massifs forestiers de l'Est algérien par la télédétection satellitaire. *International Journal of Innovation and Applied Studies*, 17(3), 954–964.

Landis, J.R. & Koch G.G. (1977). The measurement of observer agreement for categorical data. *Biometrics*, 33(1), 159–174. DOI: 10.2307/2529310.

Lu, D. & Weng Q. (2007). A survey of image classification methods and techniques for improving classification performance. *Int. J. Rem. Sens.*, 28(5), 823–870. DOI: 10.1080/01431160600746456.

Lunetta, R.S., Knight, J.F., Ediriwickrema, J., Lyon, J.G. & Worthy L.D. (2006). Land-cover change detection using multi-temporal MODIS NDVI data. *Remote Sens. Environ.*, 105(2), 142–154. DOI: 10.1016/j.rse.2006.06.018.

Malle, S.E., Tatar, H. & Boultif M. (2025). A diachronic analysis of the vegetation cover in a spate irrigation perimeter: Case study of the El Feidh Region, Biskra, Algeria. *Revue Roumaine de Géographie / Romanian Journal of Geography*, 69, 77–99. DOI: 10.59277/RRG.2025.1.06.

Metternicht, G.I. & Zinck J.A. (2003). Remote sensing of soil salinity: potentials and constraints. *Remote Sens. Environ.*, 85(1), 1–20. DOI: 10.1016/S0034-4257(02)00188-8.

Olofsson, P., Foody, G.M., Herold, M., Stehman, S.V., Woodcock, C.E. & Wulder M.A. (2014). Good practices for estimating area and assessing accuracy of land change. *Remote Sens. Environ.*, 148, 42–57. DOI: 10.1016/j.rse.2014.02.015.

Quézel, P. & Médail F. (2003). *Écologie et biogéographie des forêts du bassin méditerranéen*. Elsevier.

Rikimaru, A., Roy, P.S. & Miyatake S. (2002). Tropical forest cover density mapping. *Trop. Ecol.*, 43(1), 39–47.

Singh, A. (1989). Digital change detection techniques using remotely-sensed data. *Int. J. Remote Sens.*, 10(6), 989–1003. DOI: 10.1080/01431168908903939.

USGS. (2021). *Landsat Collection 2 Surface Reflectance Code (LaSRC)*. United States Geological Survey. <https://www.usgs.gov/landsat-missions/landsat-collection-2>

Vicente-Serrano, S.M., Quiring, S.M., Peña-Gallardo, M., Yuan, S. & Dominguez-Castro F. (2020). A review of environmental droughts: Increased risk under global warming? *Earth-Science Reviews*, 201, 102953. DOI: 10.1016/j.earscirev.2019.102953.

Zdruli, P. & Zucca C. (2023). *Restoring land and soil health to ensure sustainable and resilient agriculture in the Near East and North Africa region – State of Land and Water Resources for Food and Agriculture thematic paper*. Cairo: FAO. DOI: 10.4060/cc1137en.